

Roughness suppression via rapid current modulation on an atom chip

J.-B. Trebbia, C. L. Garrido Alzar, R. Cornelussen, C.I. Westbrook, I. Bouchoule
*Laboratoire Charles Fabry de l'Institut d'Optique, CNRS, Univ Paris-Sud,
 Campus Polytechnique, RD128, 91127 Palaiseau cedex, France*

We present a method to suppress the roughness of the potential of a wire-based, magnetic atom guide: modulating the wire current at a few tens of kHz, the potential roughness, which is proportional to the wire current, averages to zero. Using ultra-cold ^{87}Rb clouds, we show experimentally that modulation reduces the roughness by at least of a factor five without measurable heating or atom loss. This roughness suppression results in a dramatic reduction of the damping of center of mass oscillations.

PACS numbers: 39.25.+k, 03.75.Be

Atom chips, devices which trap and guide atoms with micro-fabricated structures on a substrate, hold enormous promise for the applications of cold atoms and for the exploration of new physical regimes of degenerate gases [1, 2]. For applications, their small size facilitates the design of a large variety of structures and functionalities [3, 4, 5, 6, 7]. For fundamental studies, the strong confinement possible on an atom chip permits, e.g. the study of low dimensional gases. In particular nearly one dimensional (1D) gases have been studied in the weakly interacting regime on atom chips [8, 9], and the attainment of the strongly interacting or Girardeau regime [10, 11, 12, 13, 14] on a chip is attracting significant experimental effort [15].

To exploit the full potential of these devices, atoms must often be close to the material structures they contain. This proximity however, renders atom chips highly sensitive to defects [16, 17] which produce roughness in the trapping potential. In the case of current carrying wires, most of these defects are due to the wires themselves [18, 19, 20, 21, 22]. Advances in fabrication procedures have steadily improved wire quality [23, 24], but the roughness of the trapping potential remains a problem. For example, it is a serious hindrance for the attainment of the Girardeau regime, where the atoms need to be tightly confined in the transverse direction and weakly confined in the longitudinal direction.

In this paper we demonstrate a method, first suggested in [18], which nearly eliminates the longitudinal potential roughness of a magnetic wire trap by rapid current modulation. This idea is reminiscent of the TOP trap [25] in the sense that the atoms see a time averaged potential. The wire configuration here is such that the rough potential component rapidly oscillates and averages to zero. We compare the potential roughness for unmodulated (DC) and modulated (AC) guides (with the same current amplitudes) and demonstrate a reduction factor of at least 5 without noticeable atom loss or heating. This roughness suppression results in a significant reduction of the damping of the center of mass oscillations.

A simple atomic guide can be made by a current carrying wire and a homogeneous field B_{bias} perpendicular to

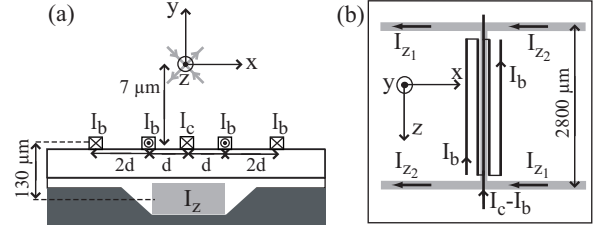


FIG. 1: Side (a) and top (b) views of the atom-chip. The first wafer (dark grey) has $15 \mu\text{m}$ thick wires (grey). On the second wafer (white), a five wire structure creates the atomic guide whose roughness is studied ($d = 2.5 \mu\text{m}$). Lengths not to scale.

the wire [1]: atoms are confined transversely and guided parallel to the wire. Atoms, of magnetic moment μ in the low field seeking state, feel a potential proportional to the absolute value of the magnetic field. The guide is centered on a line where the transverse field vanishes and the longitudinal potential $V(z)$ is given by $\mu|B_z^0 + \delta B_z^w(z)|$, where B_z^0 is an external homogeneous field, typically of one Gauss, and $\delta B_z^w(z)$ is the small, spatially fluctuating field (few mG) created by current flow deformations inside the micro-wires. Since $|B_z^0| > \delta B_z^w(z)$ and $\delta B_z^w(z)$ is proportional to the micro-wire current, current modulation around zero results in a longitudinal time-averaged potential in which the effect of $\delta B_z^w(z)$ disappears. The instantaneous position of the guide is determined by both the wire current and the transverse bias field B_{bias} . If only the wire current is modulated, the atom experiences strong forces that eliminate the transverse confinement. One must therefore also modulate B_{bias} . In our experiment, this latter field is also produced by on-chip micro wires whose low inductance permits high modulation frequencies.

We use a two layer atom chip as sketched in Fig.1. The lower silicon wafer has a H structure of $15 \mu\text{m}$ thick wires which carry the currents I_{z1} and I_{z2} . Atoms are initially loaded in an initial magnetic trap (Z-trap) [1], which is created by setting $I_{z1} = 3 \text{ A}$, $I_{z2} = 0 \text{ A}$, and applying a transverse field (in the $x - y$ plane). After evaporative

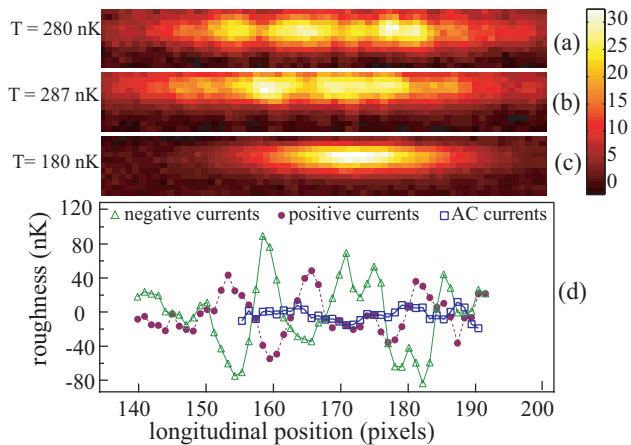


FIG. 2: (Color on line). Absorption images of a thermal cloud for negative DC (a), positive DC (b), and AC currents (c), respectively. Plotted is the number of atoms per pixel (pixel size is $6 \times 6 \mu\text{m}^2$). In (d), the potential roughnesses are extracted from longitudinal profiles using Maxwell-Boltzmann's distribution.

cooling, we have a few times 10^4 trapped ^{87}Rb atoms in the $|F = 2, m_F = 2\rangle$ state at a temperature of the order of $1 \mu\text{K}$. Next, we transfer the atomic cloud into a second trap (five-wire trap), where we perform the potential roughness measurements for both DC and AC cases. This five-wire trap is a combination of a transverse magnetic guide and a weak longitudinal confinement. The guide is realized with five parallel micro-wires ($700 \times 700 \text{ nm}^2$ and 2 mm long in the z direction) deposited on the upper silicon wafer. The wire geometry is described in [24], and shown in Fig. 1. By applying the currents $I_b = \pm 15 \text{ mA}$ in the two outer pairs of wires and $I_c = \pm 13 \text{ mA}$ in the central wire, the resulting magnetic field vanishes on a line (parallel to the z axis), $7 \mu\text{m}$ above the central wire. To prevent Majorana losses, we add a constant and homogenous longitudinal field $B_z^0 = 1.8 \text{ G}$. The weak longitudinal confinement is provided by the H-structure on the lower chip with $I_{z1} = I_{z2} = 0.4 \text{ A}$ (no current flows in the central wire of the H).

First, we measured the roughness of the trapping potential for positive and negative DC currents. After the transfer to the five-wire trap, we wait 600 ms to let the sample thermalize in the presence of an evaporative knife leading to about 5×10^3 atoms at around 280 nK . To ensure that the two DC traps have the same transverse magnetic fields to within 500 nm , we compensate the transverse magnetic fields to within 0.1 Gauss . Figures 2(a) and 2(b) show absorption images, averaged over 50 runs, of the trapped cloud at thermal equilibrium for the two DC traps. In both situations the cloud becomes fragmented, revealing the presence of potential roughness. Moreover, the density maxima and minima are inverted when the currents are reversed, as previously observed in [18]. The

time of flight (tof) for imaging is 1.5 ms . This delay allows the atoms to leave the vicinity of the five-wire structure where diffraction of the imaging beam produces systematic errors in the atomic density profile. The 1.5 ms tof of the atoms partially washes out the density modulation. This effect and the optical resolution contribute to a resolution function with a rms width of $8 \mu\text{m}$ modeled by a gaussian function. Convolution with this gaussian gives a contrast reduction of 40% for a wavelength of $60 \mu\text{m}$, the typical spatial scale observed in Fig. 2. The 10% modulation in the figure is thus an underestimate of the actual potential roughness. This smearing does not affect the relative measurements we present below, except insofar as to reduce our signal to noise ratio.

To extract the potential $V(z)$ along the guide center from the linear atomic density $n(z)$, we use the Maxwell-Boltzmann distribution $V(z) = -k_B T \ln[n(z)/n_0]$. This formula is valid because the transverse oscillation frequency is independent of z (to within 1% over the cloud extent) and provided that the phase space density is much smaller than unity. We deduce the temperature from the transverse velocity distribution measured by the standard tof technique.

The longitudinal confinement, produced by the H-shaped wire, is expected to be harmonic within 6% over the extent of the cloud. A harmonic fit of $V(z)$ gives $\omega_{z,\text{DC}}/2\pi = 7.1 \text{ Hz}$. Subtracting this potential from $V(z)$, we obtain the potential roughness plotted in Fig.2(d) for both positive and negative DC currents. The observed rms roughness amplitudes are 39 nK and 22 nK for negative and positive currents, respectively. This asymmetry in the potential roughness may be due to residual transverse magnetic fields which change the trap location, or to residual noise in the imaging system.

We now turn to the study of the AC trap. Using phase-locked oscillators at a frequency $\omega_m/2\pi = 30 \text{ kHz}$, we produce the five-wire currents $I_c(t) = \mathcal{I}_c \cos(\omega_m t)$ and $I_b(t) = \mathcal{I}_b \cos(\omega_m t)$, where $\mathcal{I}_c = 13 \text{ mA}$ and $\mathcal{I}_b = 15 \text{ mA}$ are the same currents as those used in the DC cases. The field B_z^0 and the currents I_{z1} and I_{z2} are not modulated. Loading a thermal cloud in the AC trap, the fragmentation is no longer visible in the absorption image Fig. 2(c).

To give a more quantitative analysis, we begin with a theoretical description of the AC trap. Since ω_m is much larger than all the characteristic frequencies associated with the atomic motion, the transverse and the longitudinal dynamics are described by the one cycle averaged potential $\langle V(r, t) \rangle$. Because B_z^0 is large compared to any other magnetic field, $\langle V(r, t) \rangle$ can be approximated by

$$\langle V(r, t) \rangle = \mu_B \langle |B_z(\mathbf{r}, t)| \rangle + \frac{\mu_B}{2B_z^0} \langle |\mathbf{B}_\perp^w(\mathbf{r}, t) + \mathbf{B}_\perp(\mathbf{r})|^2 \rangle. \quad (1)$$

Here, μ_B is the Bohr magneton, $B_z(\mathbf{r}, t)$ is the longitudinal magnetic field, $\mathbf{B}_\perp^w(\mathbf{r}, t)$ is the transverse magnetic field of the five wires, and $\mathbf{B}_\perp(\mathbf{r})$ denotes the transverse field created by the H wires plus any uncompensated,

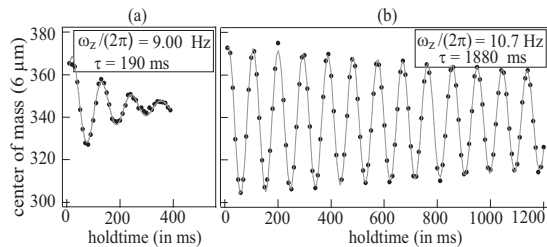


FIG. 3: Center of mass position vs time for negative DC current (a) and AC current (b) ($\omega_m/2\pi = 30$ kHz). The solid line is a fit to the function $Z(t)$ given in the text. The dramatic increase in damping time in the AC trap illustrates the strong reduction of the roughness.

homogeneous, time-independent, transverse field. Since $\delta\mathbf{B}_z^w$ oscillates, its contribution to $\langle |B_z(\mathbf{r}, t)| \rangle$ averages to zero.

The cross term $\langle \mathbf{B}_\perp^w(\mathbf{r}, t) \cdot \mathbf{B}_\perp(\mathbf{r}) \rangle$ vanishes, so that $\mathbf{B}_\perp(\mathbf{r})$ only produces a position dependent energy shift $\mu_B |\mathbf{B}_\perp(\mathbf{r})|^2 / 2B_z^0$. It has a negligible effect on the transverse confinement since the confinement created by the five-wires is very strong. On the other hand, $|\mathbf{B}_\perp(\mathbf{r})|^2$ affects the weak longitudinal confinement. The length scale on which $\mathbf{B}_\perp(\mathbf{r})$ varies is much larger than the cloud extent, because it is produced by elements located at least a millimeter away from the atomic cloud. It thus only contributes to a curvature without introducing additional roughness. The transverse magnetic field created by the H-shaped wire is $\mathbf{B}_\perp(z) = B_H z \mathbf{u}_y$, where \mathbf{u}_y is the unit vector pointing along y . This field increases the longitudinal frequency according to $\omega_{z,AC}^2 = \omega_{z,DC}^2 + \mu_B B_H^2 / (mB_z^0)$. On the other hand, the transverse frequency is reduced by $\sqrt{2}$ compared to the DC case. This factor is confirmed by our transverse frequency measurements which give (1.2 ± 0.2) kHz for the AC trap, (2.2 ± 0.1) kHz and (2.1 ± 0.1) kHz for DC negative and positive currents, respectively.

We extract the potential in the AC trap from the measured longitudinal profile for a sample at $T = 180$ nK. From a harmonic fit we obtain a longitudinal frequency of 11.3 Hz, slightly larger than the one in the DC trap, as expected. In Fig.2(d), we compare the measured roughness of the AC trap to those obtained in the DC traps. In the AC configuration, the roughness rms amplitude is reduced by a factor 4 and 7 with respect to the positive and negative DC cases. The residual apparent roughness in the AC case is consistent with the noise in the imaging system and so the mean reduction factor of 5 is a lower limit.

We also tested the reduction of the potential roughness by looking at the evolution of the longitudinal center of mass oscillations (CMO) as shown in Fig.3. In a harmonic trap, the CMO of an atomic cloud are undamped. In the presence of a potential roughness, the oscillation period depends on the amplitude and the de-

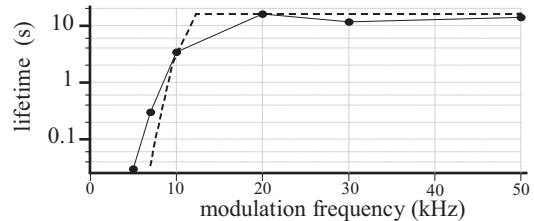


FIG. 4: Lifetime vs. ω_m in the AC trap (dots). The dashed line represents the result of Monte Carlo calculations with a transverse magnetic field of 150 mG for both x and y directions.

phasing between trajectories of different particles results in a damping of the CMO. Figure 3 shows the dramatic contrast between the AC and DC traps. We fit the oscillations to the function $Z(t) = Z_0 + Z_1 e^{-t^2/\tau^2} \cos(\omega t + \phi)$, where Z_0 , Z_1 , τ , ω and ϕ are fitting parameters. This function ensures the expected quadratic decrease of the oscillation amplitude at small times for a damping due to trajectory dephasing. The fitted damping time in the AC case, $\tau = (1.9 \pm 0.1)$ s, is ten times larger than its value in the DC case. In fact, the observed damping in the AC guide can be explained by the anharmonicity of the H-shaped wire confinement alone. Thus, the data are consistent with the absence of roughness.

To estimate an upper bound on the ratio of the AC to DC roughness amplitudes, we performed one dimensional classical Monte Carlo calculations for non-interacting atoms experiencing a rough potential superimposed on a harmonic confinement. The calculations are averaged over potential roughness realizations with the spectral density expected for a single wire having white noise border deformations [22, 26]. We adjust the wire border noise in order to recover the measured damping time in the DC trap (it corresponds to an rms roughness of 80 nK). We find that the observed increase of the damping time by a factor 10 requires a reduction of the potential roughness by about 14. A drawback of the model is that it does not take into account atomic collisions, happening at a rate on the order of the damping time. However, as collisions are present in both the DC and AC configurations, we assume that the above roughness reduction deduced from the calculation is still relevant.

The modulation technique does not correct for all guide defects. By considering only the time-averaged potential we neglect the micro-motion of the atoms [27] whose energy is responsible for a residual roughness. This roughness is 10^{-8} times smaller than the one present in the DC guides for our experimental parameters. In fact, other imperfections are more important. First, the transverse component of the rough micro-wire field produces mean-
ders of the guide equipotentials (displacement of about 2 nm) and a z -dependent modification of the transverse

trapping frequency (approximately 0.3%). These two effects are not averaged out in the AC guide. Second, the rough longitudinal field $\delta\mathbf{B}_z^w$ appears in the expansion of $\langle V(r, t) \rangle$ to orders that are neglected in Eq. (1). The resulting guide imperfections are one order of magnitude smaller than those produced by the transverse component of the rough field.

We also investigated the dependence of the trap lifetime on ω_m as shown in Fig.4. For modulation frequencies above 15 kHz, the lifetime of the sample is the same as in the DC case. For lower modulation frequencies, we observe a decrease in lifetime that we attribute to instabilities of the atomic trajectories in the modulated potential. For zero unmodulated transverse magnetic field $\mathbf{B}_\perp(\mathbf{r})$, the transverse atomic motion close to the guide center is governed by the Mathieu equation [27] and no instabilities are expected for $\omega_m > 0.87\omega_{\perp,DC}$, where $0.87\omega_{\perp,DC}/2\pi = 1.82$ kHz which is significantly below 15 kHz. We attribute this discrepancy to the presence of a non vanishing transverse field. Classical trajectory Monte Carlo simulations, with fields of 150 mG in both x and y directions, reproduce well the measured lifetime as shown in Fig. 4 (dashed line). This value is of the same order as the accuracy of the residual transverse field compensation. Within the explored range of frequencies (up to 50 kHz), we have not identified any upper bound for the modulation frequency. The atomic spin should adiabatically follow the magnetic field orientation to avoid spin flip losses. This condition is fulfilled provided that $\omega_m/2\pi \ll \mu_B B_z^0/4\pi\hbar$, where $\mu_B B_z^0/4\pi\hbar \simeq 1.3$ MHz is the Larmor frequency.

The temporal modulation of the rough potential can lead to a heating [28]. In our trap however, the expected heating rate is very small. This is confirmed by our measured heating rate of about 160 nK/s which is close to the technical heating, also observed in the DC trap. We have also loaded a Bose-Einstein condensate in the AC trap without noticeable fragmentation.

The method presented here will enable new experimental explorations on quantum gases using atom chips. We have already mentioned the study of a 1D Bose gas in the Girardeau regime. Note that the reduction of transverse trapping frequency by $\sqrt{2}$ can be overcome by going closer to the wire. Second, the relative insensitivity of the time-averaged potential to residual transverse magnetic fields will enable us to revisit proposals of double well potentials in static magnetic fields, such as [19, 24], which are very sensitive to residual magnetic fields. Finally, this method may also allow the study of atom dynamics

in disordered potentials [29, 30, 31] since the roughness strength can be tuned.

The authors thank A. Aspect, T. Schumm and J. Estève for fruitful discussions. The Atom Optics group of Laboratoire Charles Fabry is a member of the IFRAF Institute. This work was supported by the EU under grants No. MRTN-CT-2003-505032 and No. IP-CT-015714.

-
- [1] R. Folman *et al.*, Adv. At. Mol. Opt. Phys. **48**, 263 (2002), and references therein.
 - [2] European Physical Journal D **35**, (2005), special issue on atom-chips.
 - [3] W. Hänsel, J. Reichel, P. Hommelhoff, and T. W. Hänsch, Phys. Rev. Lett. **86**, 608 (2001).
 - [4] A. Günther *et al.*, Phys. Rev. Lett. **95**, 170405 (2005).
 - [5] Y.-J. Wang *et al.*, Phys. Rev. Lett. **94**, 090405 (2005).
 - [6] T. Schumm *et al.*, Nature Physics **1**, 57 (2005).
 - [7] P. Treutlein *et al.*, Phys. Rev. Lett. **92**, 203005 (2004).
 - [8] J. Estève *et al.*, Phys. Rev. Lett. **96**, 130403 (2006).
 - [9] J.-B. Trebbia, J. Estève, C. I. Westbrook, and I. Bouchoule, Phys. Rev. Lett. **97**, 250403 (2006).
 - [10] M. Girardeau, J. Math. Phys. **1**, 516 (1960).
 - [11] B. L. Tolra *et al.*, Phys. Rev. Lett. **92**, 190401 (2004).
 - [12] B. Parades *et al.*, Nature **429**, 277 (2004).
 - [13] H. Moritz, T. Stöferle, M. Köhl, and T. Esslinger, Phys. Rev. Lett. **91**, 250402 (2003).
 - [14] T. Kinoshita, T. Wenger, and D. S. Weiss, Science **305**, 1125 (2004).
 - [15] J. Reichel and J. H. Thywissen, J. Phys. IV France **116**, 265 (2004).
 - [16] B. V. Hall *et al.*, J. Phys. B **39**, 27 (2006).
 - [17] C. D. J. Sinclair *et al.*, Phys. Rev. A **72**, 031603 (2005).
 - [18] S. Kraft *et al.*, J. Phys. B **35**, L469 (2002).
 - [19] M. A. Jones *et al.*, J. Phys. B **37**, L15 (2004).
 - [20] A. E. Leanhardt *et al.*, Phys. Rev. Lett. **90**, 100404 (2003).
 - [21] J. Estève *et al.*, Phys. Rev. A **70**, 043629 (2004).
 - [22] D.-W. Wang, M. D. Lukin, and E. Demler, Phys. Rev. Lett. **92**, 076802 (2004).
 - [23] L. D. Pietra *et al.*, J. Phys.: Conf. Ser. **19**, 30 (2005).
 - [24] J. Estève *et al.*, Eur. Phys. J. D **35**, 141 (2005).
 - [25] W. Petrich, M. H. Anderson, J. R. Ensher, and E. A. Cornell, Phys. Rev. Lett. **74**, 3352 (1995).
 - [26] T. Schumm *et al.*, Eur. Phys. J. D **32**, 171 (2005).
 - [27] L. Landau and E. Lifshitz, *Mechanics, Fourth Edition, Course of Theoretical physics* (MIR Editions, Moscow, 1982).
 - [28] I. Bouchoule *et al.*, in preparation.
 - [29] D. Clément *et al.*, Phys. Rev. Lett. **95**, 170409 (2005).
D. Clément *et al.*, New Journal of Phys. **8**, 165 (2006).
 - [30] T. Schulte *et al.*, Phys. Rev. Lett. **95**, 170411 (2005).
 - [31] J. E. Lye *et al.*, Phys. Rev. Lett. **95**, 070401 (2005).